Title:
The Comprehensive Diagnostic Transesophageal Echocardiogram: Integrating 2D and 3D Imaging, Doppler Quantitation and Advanced Approaches

Words: 8600
Tables: 8
Figures: 23

Rosario V. Freeman, MD MS
Director, Cardiology Fellowship Programs
University of Washington, Box 356422
Seattle, WA 98195
rosariof@u.washington.edu
Assistant (Sally) 206-685-1397

Table 1. Appropriate indications for TEE as a diagnostic test.
Adapted from Douglas, et al.[1]

| |
|---|
| **Appropriate** |
| Use of TEE when there is a high likelihood of a non-diagnostic TTE due to patient characteristics or inadequate visualization of relevant structures |
| Re-evaluation of prior TEE finding for interval change when a change in therapy is anticipated |
| Guidance during percutaneous non-coronary cardiac interventions including but not limited to closure device placement, radiofrequency ablation, and percutaneous valve procedures |
| Suspected acute aortic pathology including but not limited to dissection/transection. |
| Evaluation of valve structure and function to assess suitability for, and assist in planning of, an intervention |
| To diagnose infective endocarditis with a moderate or high pretest |
| Evaluation for cardiovascular source of embolus with no identified non-cardiac source |
| Evaluation to facilitate clinical decision making with regards to anticoagulation, cardioversion, and/or radiofrequency ablation |
| **Uncertain** |
| Evaluation for cardiovascular source of embolus with a previously identified non-cardiac source |
| **Inappropriate** |
| Routine use of TEE when a diagnostic TTE is reasonably anticipated to resolve all diagnostic and management concerns |
| Surveillance of prior TEE finding for interval change when no change in therapy is anticipated |
| Routine assessment of pulmonary veins in an asymptomatic patient status post pulmonary vein isolation |
| To diagnose infective endocarditis with a low pretest probability |
| Evaluation for cardiovascular source of embolus with a known cardiac source in which a TEE would not change management |
| Evaluation when a decision has been made to anticoagulate and not to perform cardioversion |

Table 2. Technical skills necessary for performance of TEE.
Adapted from Quinones, et al.[7]

| |
|---|
| Uses conscious sedation safely and effectively. |
| Performs a complete TTE exam, using all echocardiographic modalities relevant to the case. |
| Safely passes TEE probe into the esophagus and stomach, and adjusts probe position to obtain necessary tomographic images and Doppler data. |
| Operates ultrasonographic instrument correctly, including controls affecting quality of displayed data. |
| Recognizes abnormalities of cardiac structure and function detected from TEE images, distinguishes normal from abnormal findings, and recognizes artifacts. |
| Performs qualitative and quantitative analyses of echocardiographic data. |
| Produces a cogent written report of echocardiographic findings and their clinical implications. |

Table 3. Clinical features associated with increased risk respiratory compromise during moderate conscious sedation

| |
|---|
| Airway patency – prior history of airway management problems, obstructive sleep apnea, small mouth opening, significant malocclusion |
| Elderly patients – Increased sensitivity to sedatives and higher incidence of interactions of with other medications |
| Congestive heart failure – Severe LV systolic dysfunction, critical aortic stenosis |
| Underlying respiratory disease – oxygen dependency, severe pulmonary hypertension/cor pulmonale |
| Neurologic or neuromuscular disorders compromising respiratory or swallowing, inability to follow commands |
| Non-fasting state |

Table 4. Risk of complications for TEE.
Adapted from Hilberath et al.[14]

| **Complication** | **Rate (%)** |
|---|---|
| Mortality | <0.01-0.02 |
| Esophageal perforation | <0.01 |
| Major bleeding | <0.01 |
| Minor bleeding | 0.01-0.2 |
| Bronchospasm | 0.07 |
| Dental injury | 0.1 |
| Arrhythmia | 0.06-0.3 |
| Dental injury | 0.1 |
| Dysphagia | 1.8 |
| Hoarseness | 12 |
| Lip injury | 13 |

Table 5. Standard TEE views

| View | Transducer angle +/- ~10° each view |
|---|---|
| **Mid-esophageal (ME) views** | |
| [1] ME 5-chamber view | 0° |
| [2] ME 4-chamber view | 10° |
| [3] ME mitral commissural view | 60° |
| [4] ME 2-chamber view | 90° |
| [5] ME LV long-axis view | 130° |
| [6] ME AV long-axis view | 130° |
| [7] ME right pulmonary vein view | 10° |
| [8] ME AV short-axis view | 40° |
| [9] ME RV inflow-outflow view | 70° |
| [10] ME bicaval TV view | 70° |
| [11] ME bicaval view | 100° |
| [12] ME left atrial appendage | 90° |
| **Upper-esophageal (UE) views** | |
| [13] UE ascending aorta long-axis view | 100° |
| [14] UE ascending aorta short-axis view | 30° |
| [15] UE pulmonary veins view | 90° |
| **View** | **Transducer angle +/- ~10° each view** |
| **Transgastric (TG) views** | |
| [16] TG LV basal short-axis view | 0° |
| [17] TG LV mid-papillary short-axis view | 0° |
| [18] TG LV apical short-axis view | 0° |
| [19] TG RV basal view | 0° |
| [20] TG RV inflow-outflow view | 0° |
| [21] TG 2-chamber view | 90° |
| [22] TG LV long-axis view | 120° |
| [23] TG RV inflow view | 90° |
| [24] Deep TG LV view | 0° |
| **Aortic views** | |
| [25] ME aorta descending short-axis view | 0° |
| [26] ME aorta descending long-axis view | 90° |
| [27] UE aortic arch long-axis view | 0° |
| [28] UE aortic arch short-axis view | 90° |

ME – mid-esophageal, UE – upper esophageal, TG – transgastric, LV – left ventricle, RV – right ventricle, AV – aortic valve

Table 6. Standard TEE views for cardiac structures: Cardiac chambers and great vessels

| Structure | View | Transducer angle, probe position |
|---|---|---|
| ***Cardiac chambers*** | | |
| Left ventricle | [2] ME 4-chamber view | 10°, tip leftward and retroflexed |
| | [4] ME 2-chamber view | 90° |
| | [5] ME LV long-axis view | 130° |
| | [17] TG LV mid-papillary short-axis view | 0°, anteflexed |
| | [21] TG 2-chamber view | 90° |
| | [24] Deep TG LV view | 0° |
| | 3D echocardiography | Entire LV in imaging sector |
| Left atrium | [2] ME 4-chamber view | 10°, decreased depth |
| | [4] ME 2-chamber view | 90° |
| | [5] ME LV long-axis view | 130° |
| Left atrial appendage | [12] ME left atrial appendage | 90°, biplane imaging |
| Pulmonary veins | [15] UE pulmonary veins view | 90°, tip rightward for right PV |
| | [7] ME right pulmonary vein view | 10°, or tip leftward for left PV |
| Right ventricle | [2] ME 4-chamber view | 10°, tip rightward |
| | [9] ME RV inflow-outflow view | 70° |
| | [20] TG RV inflow-outflow view | 0°, tip rightward |
| | [23] TG RV inflow view | 90° |
| Right atrium | [2] ME 4-chamber view | 10°, decreased depth |
| | [23] TG RV inflow view | 90° |
| Inter-atrial septum | [11] ME bicaval view | 100°, tip rightward |
| | 3D echocardiography | 100°, decreased depth |
| ***Great vessels*** | | |
| Ascending aorta | [6] ME AV long-axis view | 130° |
| | [13] UE ascending aorta long-axis view | 100°, tip rightward |
| | [14] UE ascending aorta short-axis view | 30° |
| Descending aorta | [25] ME aorta descending short-axis view | 0° |
| | [26] ME aorta descending long-axis view | 90° |
| | [27] UE aortic arch long-axis view | 0° |
| | [28] UE aortic arch short-axis view | 90° |
| Pulmonary artery | [9] ME RV inflow-outflow view | 70°, probe to UE, tip rightward |
| | [28] UE aortic arch short-axis view | 90° |

ME – mid-esophageal, UE – upper esophageal, TG – transgastric, LV – left ventricle, RV – right ventricle, AV – aortic valve, PV – pulmonary veins

Table 7. Standard TEE views for cardiac structures: Cardiac valves

| **Structure** | **View** | **Probe position, Tip placement** |
|---|---|---|
| ***Valves*** | | |
| Mitral valve | [2] ME 4-chamber view | 10° |
| | [3] ME mitral commissural view | 60° |
| | [5] ME LV long-axis view | 130° |
| | [16] TG LV basal short-axis view | 0°, enface image, anteflexed |
| | 3D echocardiography | Zoomed enface image, rotate to AV at top of display |
| Aortic valve | [1] ME 5-chamber view | 0°, anteflexed |
| | [6] ME AV long-axis view | 130° |
| | [8] ME AV short-axis view | 40°, anteflexed |
| | [22] TG LV long-axis view | 120° |
| | 3D echocardiography | Zoomed enface image, rotate to right cusp at bottom of display |
| Tricuspid valve | [2] ME 4-chamber view | 10° |
| | [9] ME RV inflow-outflow view | 70° |
| | [10] ME bicaval TV view | 70° |
| | [19] TG RV basal view | 0°, enface image |
| | [23] TG RV inflow view | 90° |
| | 3D echocardiography | Zoomed enface image |
| Pulmonic valve | [9] ME RV inflow-outflow view | 70° |

ME – mid-esophageal, TG – transgastric, LV – left ventricle, RV – right ventricle, AV – aortic valve

Table 8. Components and proposed sequence of a comprehensive TEE study

| | Sequence | Comments |
|---|---|---|
| | ***Mid-esophageal views*** | |
| 1. | Evaluate primary study indication | Endocarditis evaluation, cardiac source of embolus, acute aortic syndrome, etc. |
| 2. | Left ventricular size and function | Depth to include entire LV. Transducer angle 0°-130° Global and regional function, 3DE LV volumes and EF |
| 3. | Right ventricular size and function | Depth to include entire RV. Transducer angle 0°-70° |
| 4. | Left atrium | Decrease depth to below MV. Sweep across the atrium at transducer angles between 0°-90°. |
| 5. | Left atrial appendage | Biplane imaging. Adjust position to decrease artifact from ridge between LUPV and LAA. Pulse wave Doppler of velocities for atrial fibrillation. |
| 6. | Right atrium | Decrease depth to just below mitral valve. Sweep across the atrium at transducer angles between 0°-90° |
| 7. | Mitral valve | 2D imaging and color Doppler from multiple views, transducer angle 0°-130°. Quantitation of regurgitation severity, vena contracta and PISA EROA calculation for more than mild regurgitation. Mitral inflow gradient for stenosis. 3DE enface view of valve rotated to aortic valve at top of display. |
| 8. | Aortic valve | 2D imaging and color Doppler from multiple views, transducer angle 0°-130°. Vena contracta for more than mild regurgitation. 3DE enface view of valve rotated to right coronary cusp at bottom of display. |
| 9. | Ascending aorta (Upper esophageal) | Transducer angle 100°. Measure if dilated (sinuses, sinotubular junction, mid-ascending aorta) |
| 10. | Tricuspid valve | 2D imaging and color Doppler from multiple views, transducer angle 0°- 60°. |
| 11. | Pulmonic valve | 2D imaging and color Doppler, transducer angle 70°. |
| 12. | Inter-atrial septum and bicaval view | 2D imaging and color Doppler at lower Nyquist setting, transducer angle 100°. If shunt suspected, 3DE enface view and agitated saline contrast study. If present, evaluate |
| 13. | Pulmonary veins | 2D imaging and color Doppler, transducer angle 0° and 100° for left and right pulmonary veins. Pulse wave Doppler if significant MR, to evaluate for flow reversal. |
| 15. | Pericardial space | Sweep across the heart at a transducer angle 0° |
| | ***Transgastric views*** | |
| 16. | Ventricular function | Evaluate biventricular size and function, transducer angle 0° and 120°. Rotate probe tip rightward for RV and tricuspid valve. Enface view of MV with color Doppler if significant MR. |
| 17. | Deep transgastric view | Advance probe from transgastric view. Visualize LV outflow for Doppler interrogation if needed. |
| | ***Aorta view*** | |
| 18. | Descending thoracic aorta | Image from the diaphragm to the aortic arch. Biplane imaging, 0° and 90°. Pulse wave Doppler if significant AR, to evaluate for flow reversal. Image atherosclerotic plaque. |

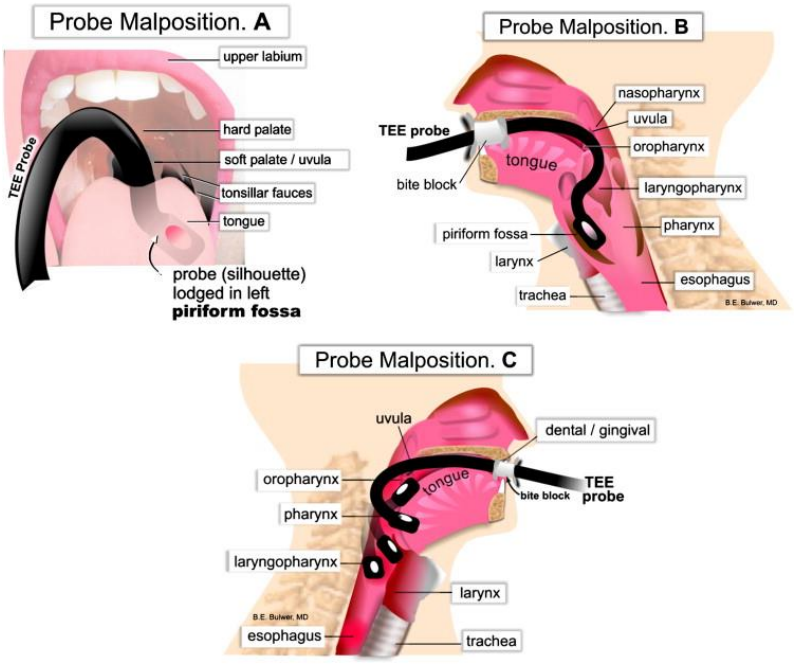


Figure 1. Probe malposition. **(A,B)** Difficulty during probe insertion can be encountered if the TEE probe is lodged into one of the piriform sinuses. **(C)** In addition to causing mucosal injury to the oropharynx, the TEE probe can occasionally become distorted in extreme flexion. From Hilberath et al (figure 2).[14]

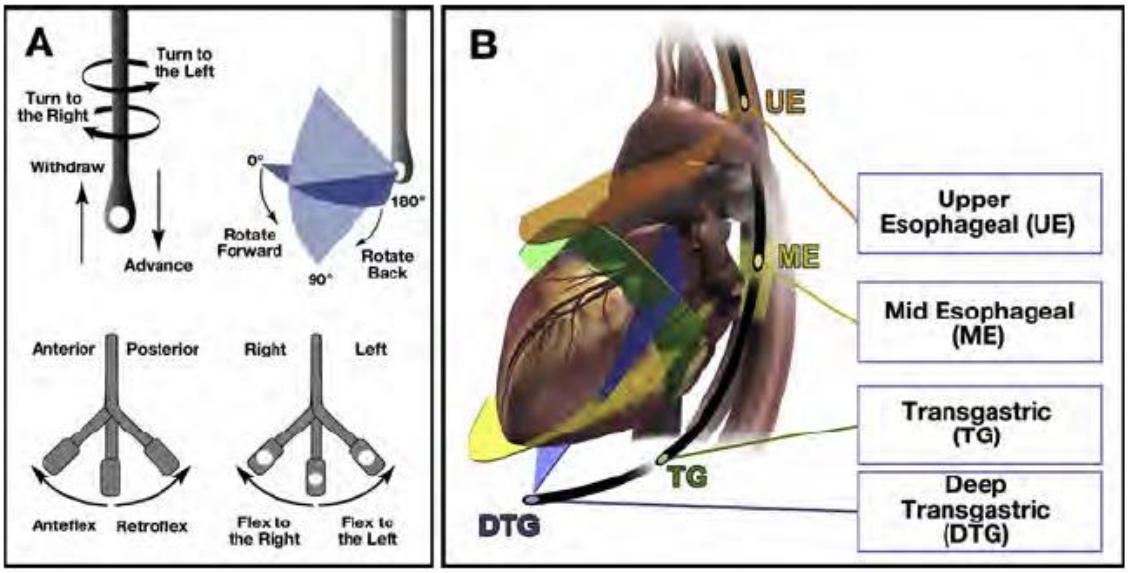

Figure 2. Probe manipulation (left) and esophageal position (right). A button on the probe handle electronically controls the transducer angle. Controls on the handle allow manipulation of the probe tip with anteflextion/retroflextion (larger control knob), and right/left flexion (smaller control knob). From Hahn et al (figure 2).[19]

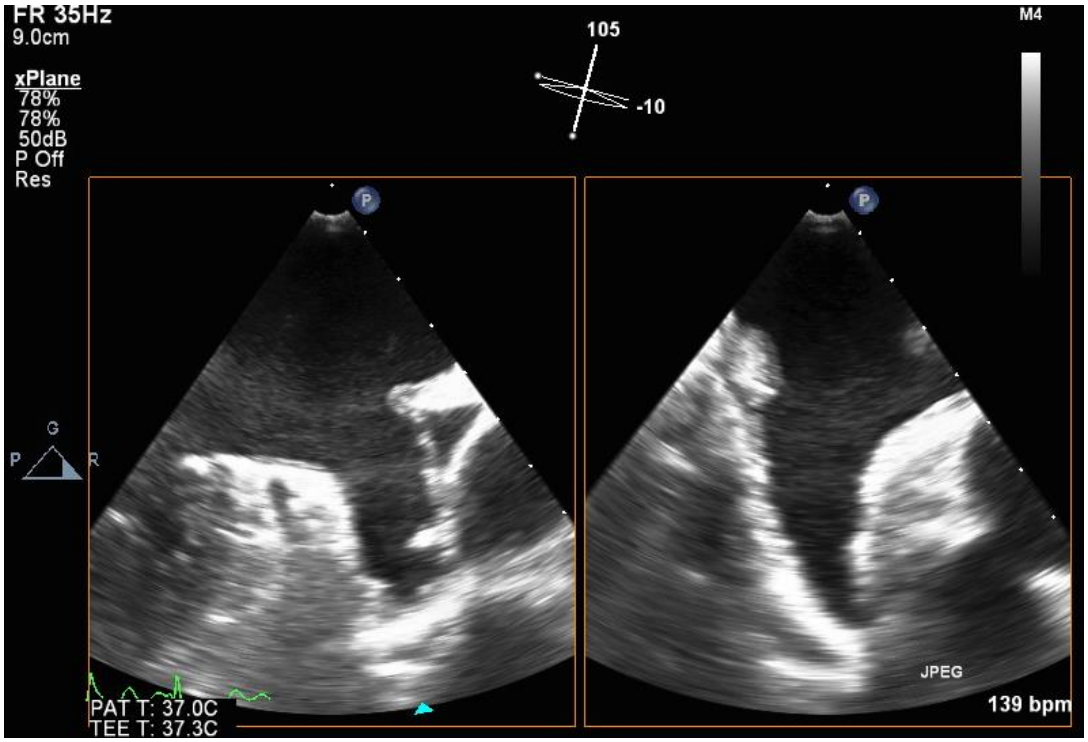


Figure 3. [View 12] Biplane image of the left atrial appendage. The primary image (left side of display), and the secondary image in a perpendicular plane (right) is simultaneously displayed.

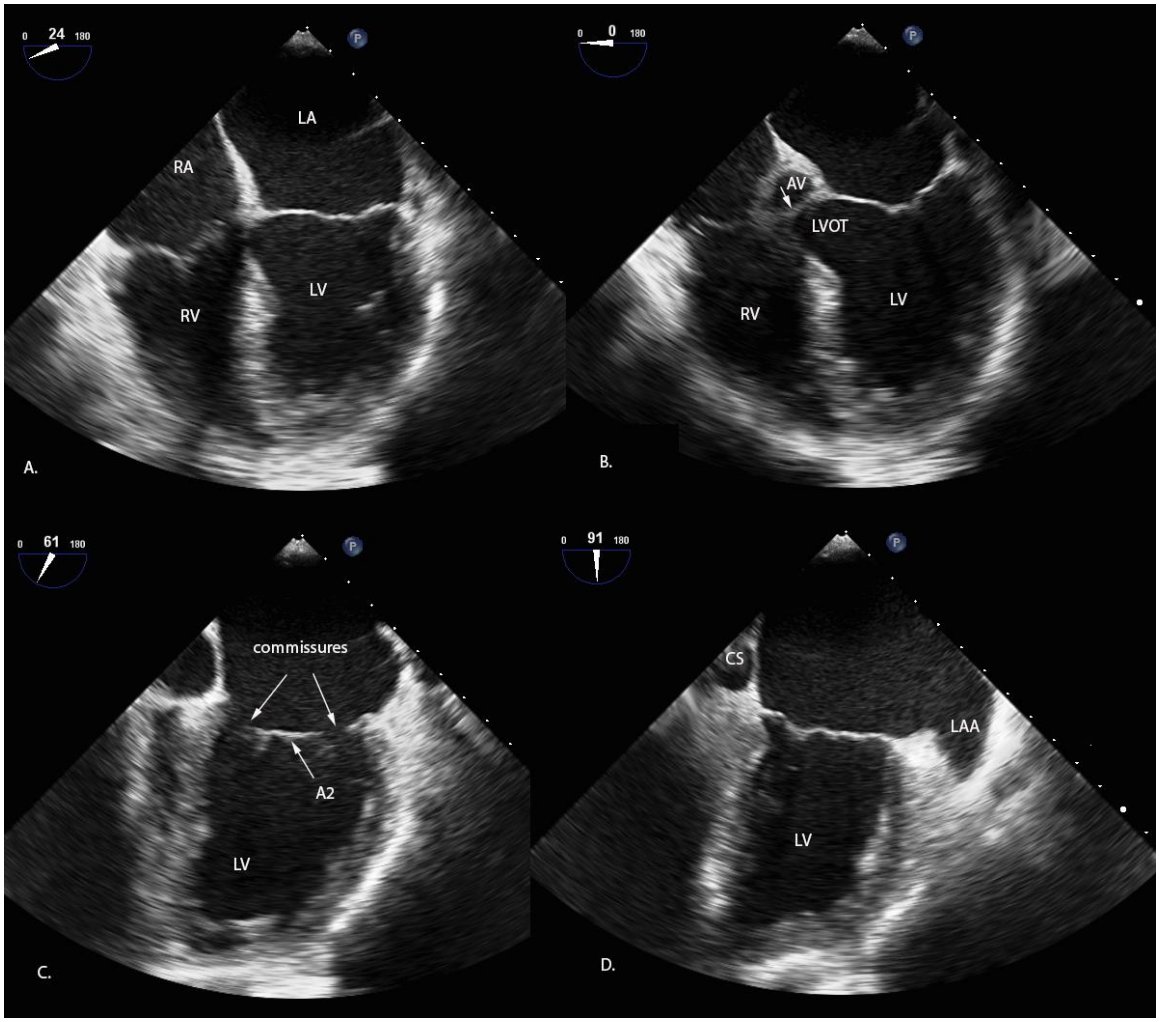


Figure 4. The left ventricular views. [View 2] Mid-esophageal 4-chamber view, Panel A: the atria (LA, RA) are in the near field, and the ventricles (LV, RV) are in the far field. [View 1] Mid-esophageal 5-chamber view, Panel B: with the probe tip slightly anteflexed, the left ventricular outflow tract (LVOT) and aortic valve (AV) are seen. [View 3] Mid-esophageal mitral commissural view, Panel C: the mid-portion of the anterior mitral valve leaflet (A2 segment) is seen with commissures on either side of the segment. [View 4] Mid-esophageal 2-chamber view, Panel D: the left atrial appendage (LAA) is on the right side of the display, and the coronary sinus (CS) is on the left side of the image.

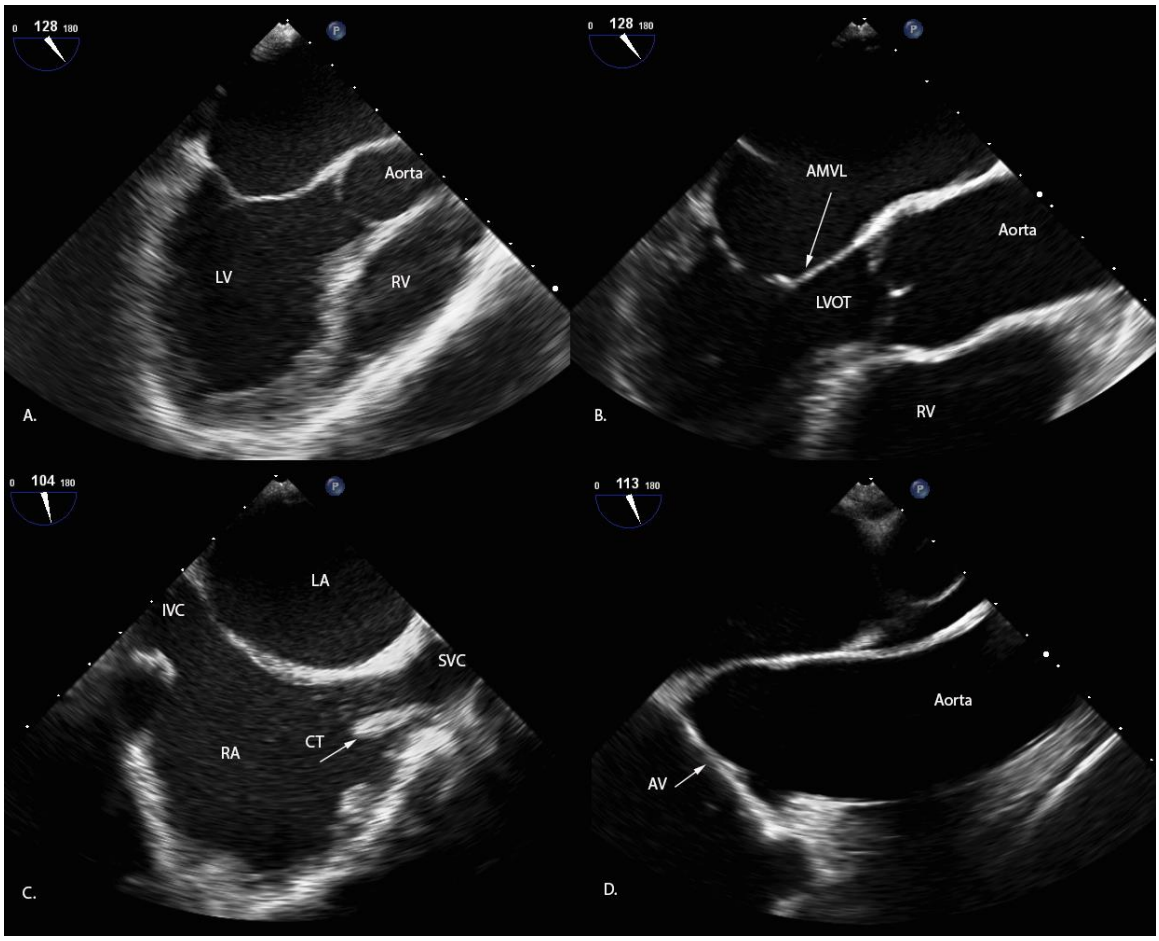


Figure 5. Left ventricular long axis, proximal aorta, and bicaval views. [View 5] Mid-esophageal left ventricular long axis view, Panel A: the LV and aortic valve are seen, with a portion of the RV in the far field, towards the right side of the image. [View 6] Mid-esophageal aortic valve long-axis view, Panel B: the anterior mitral valve leaflet (AMVL) is adjacent to the posterior aspect of the aortic valve; this is obtained by decreasing the depth from the LV long axis view and rotating the probe slightly so the aortic valve is in the center of the sector. [View 13], Panel D: upper-esophageal ascending aorta long-axis view. [View 11] Mid-esophageal bicaval view, Panel C: the LA is in the near field with the inter-atrial septum bisecting the imaging sector. The superior vena cava (SVC) drains on the right side of the display. Adjacent to the SVC is the crista terminalis (CT).

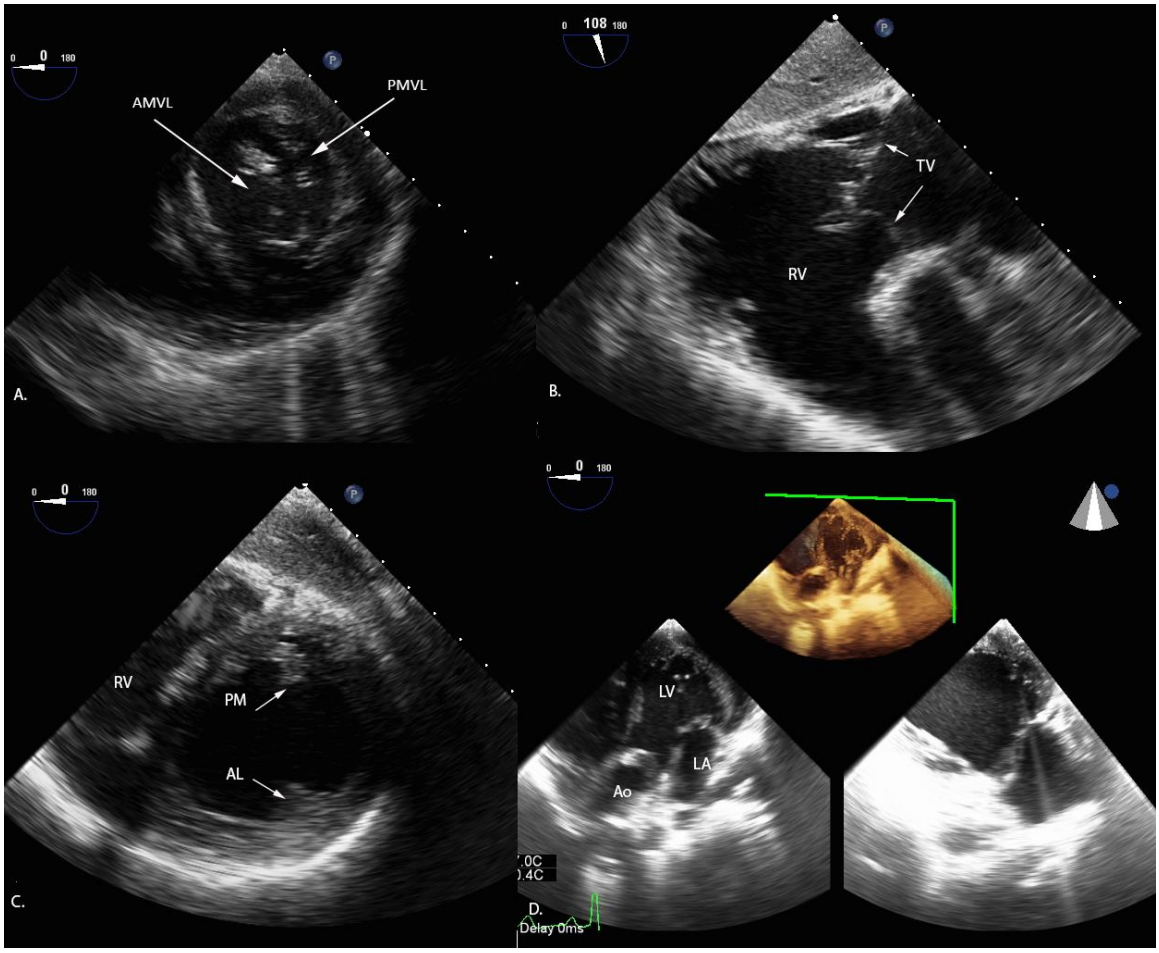


Figure 6. Transgastric views. [View 16], Panel A: transgastric mitral valve short-axis view. The anterior mitral valve leaflet (AMVL) is on the left side of the display, and the posterior mitral valve leaflet (PMVL) is on the right. [View 23], Panel B: transgastric right ventricular inflow view. The right ventricle (RV) is on the left side of the display, and the right atrium is on the right side of the display. [View 17], Panel C: transgastric LV mid-papillary short-axis view. The inferior wall and the posteromedial (PM) papillary muscle are in the near field, and the anterior wall and anterolateral (AL) papillary muscle are in the far field. [View 24], Panel D: biplane imaging of the LV from a deep gastric position. The LV is in the near field, with the aortic valve in the far field. The orthogonal view of the left ventricle is concurrently displayed on the right side of Panel D.

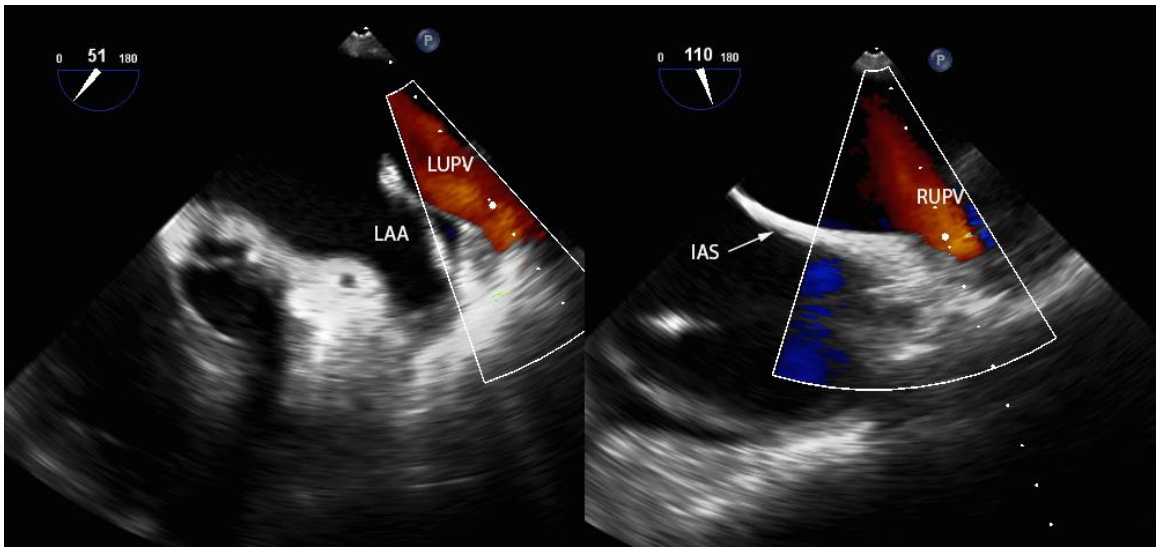


Figure 7. [View 15] Upper-esophageal pulmonary veins view. The right upper pulmonary vein (RUPV) (right image) is adjacent to the inter-atrial septum. The left pulmonary vein (LUPV) (left image), is adjacent to the left atrial appendage, although in some cases may be seen better at a lower transducer angle from 90°, in this case, at 51°.

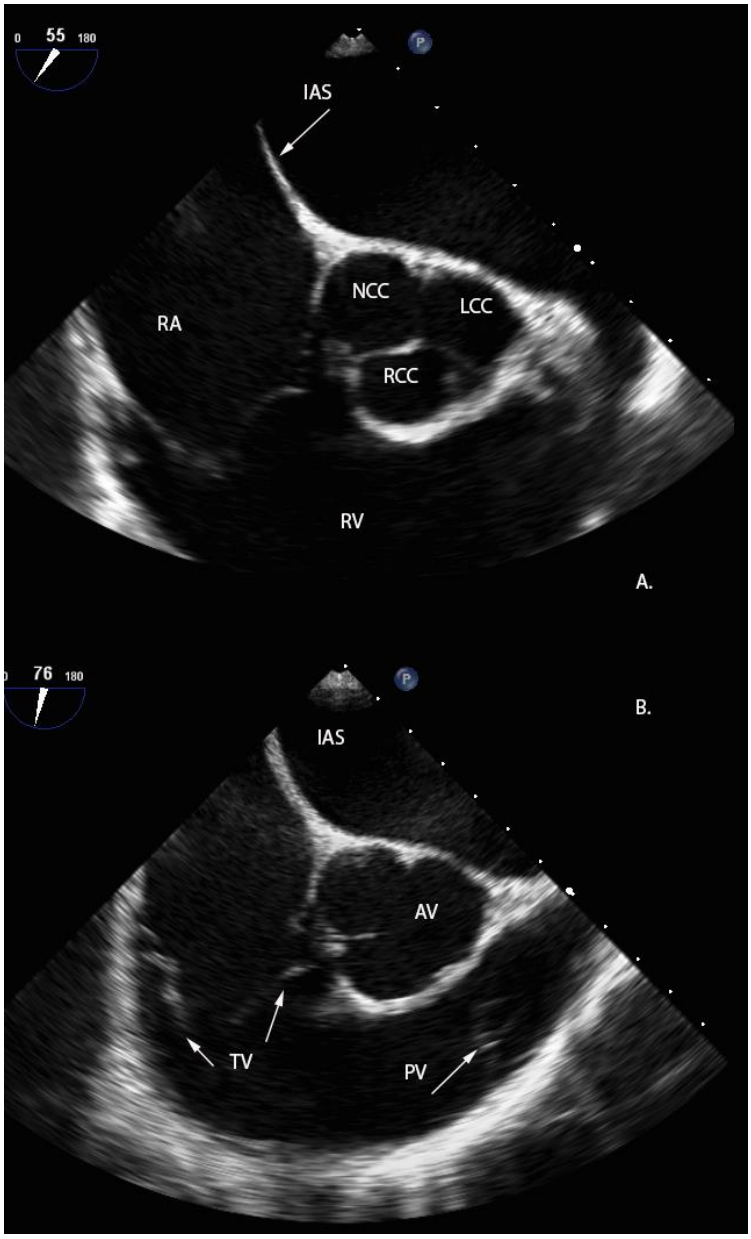


Figure 8. [View 8], Panel A. Mid-esophageal aortic valve short axis view. The non-coronary cusp (NCC) is bisected by the inter-atrial septum (IAS), and the right coronary cusp (RCC) is adjacent to the RV. [View 9], Panel B. Mid-esophageal right ventricular inflow-outflow view. The pulmonic valve (PV) is in the far field at the right side of the display.

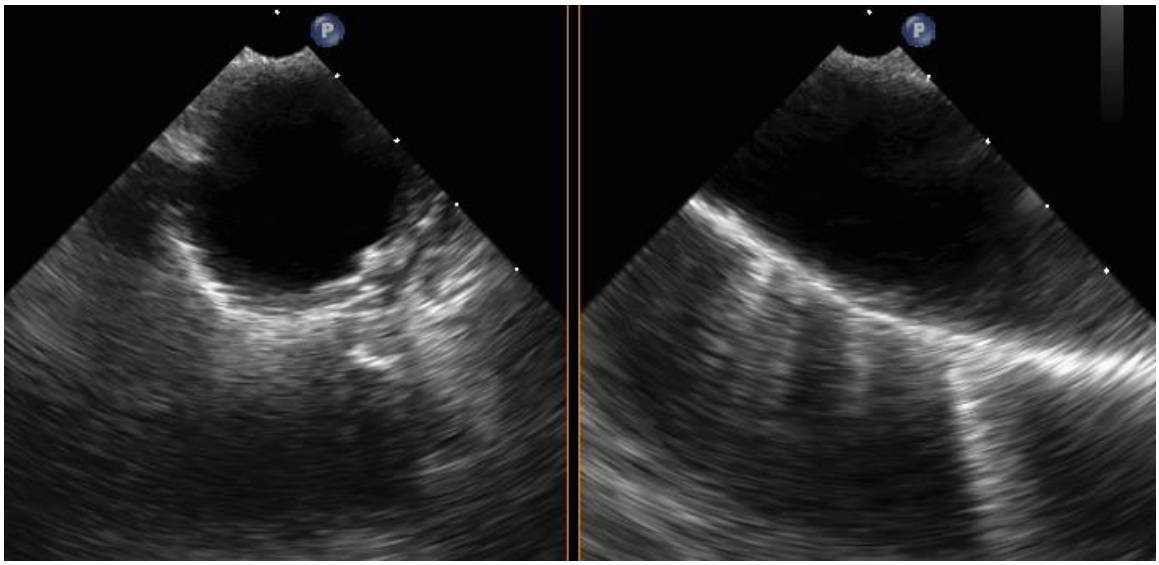

Figure 9. Biplane image acquisition of the mid-esophageal descending aorta short-axis view (0°)[View 25](left), and the mid-esophageal descending aorta long-axis view (90°)[View 26](right).

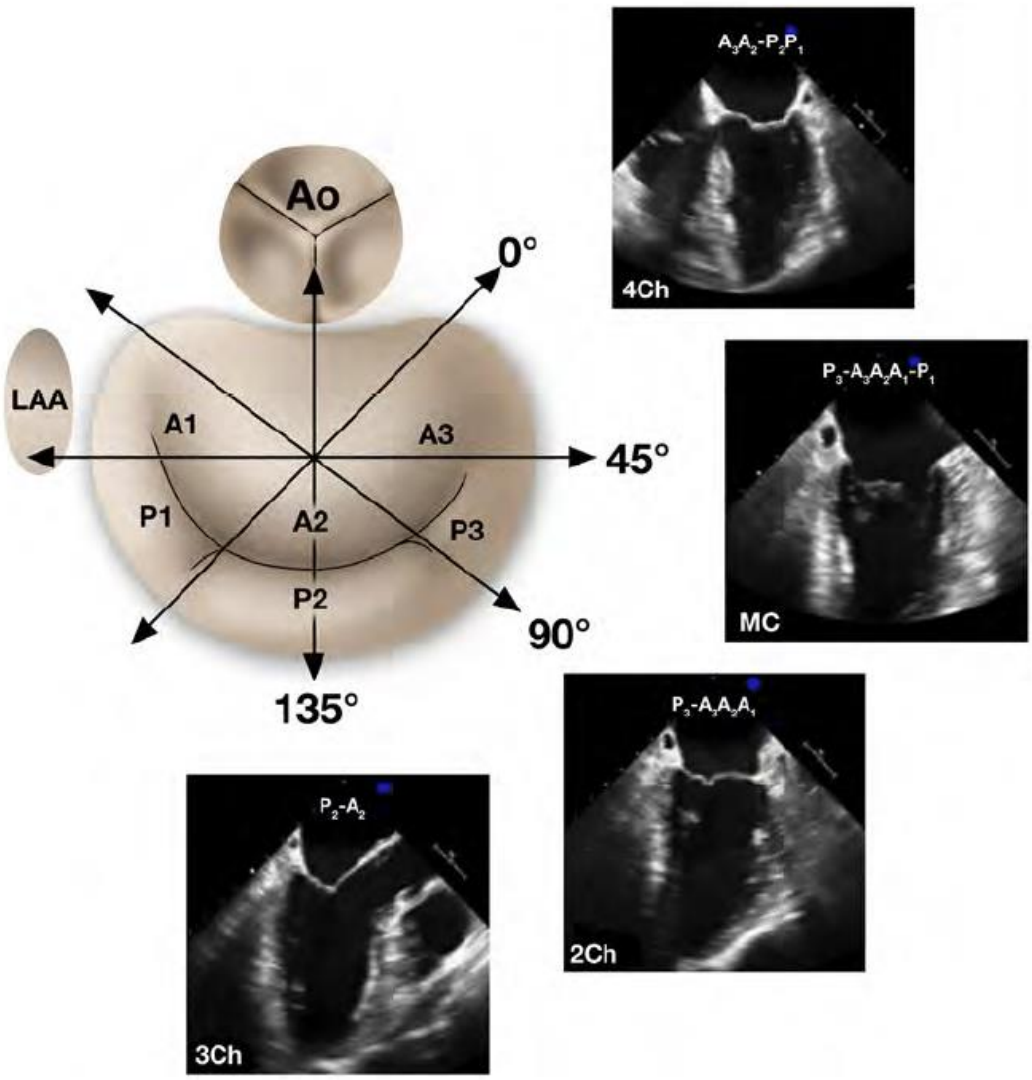


Figure 10. Schematic of the mitral valve with labeled segments. At each transducer angle, a corresponding image from that view is shown. Anatomic variability and probe placement may slightly vary the exact mitral segment imaged. LAA (left atrial appendage), Ao (aortic valve), Ch (chamber), MC (mitral commissural). From Hahn et al.[19]

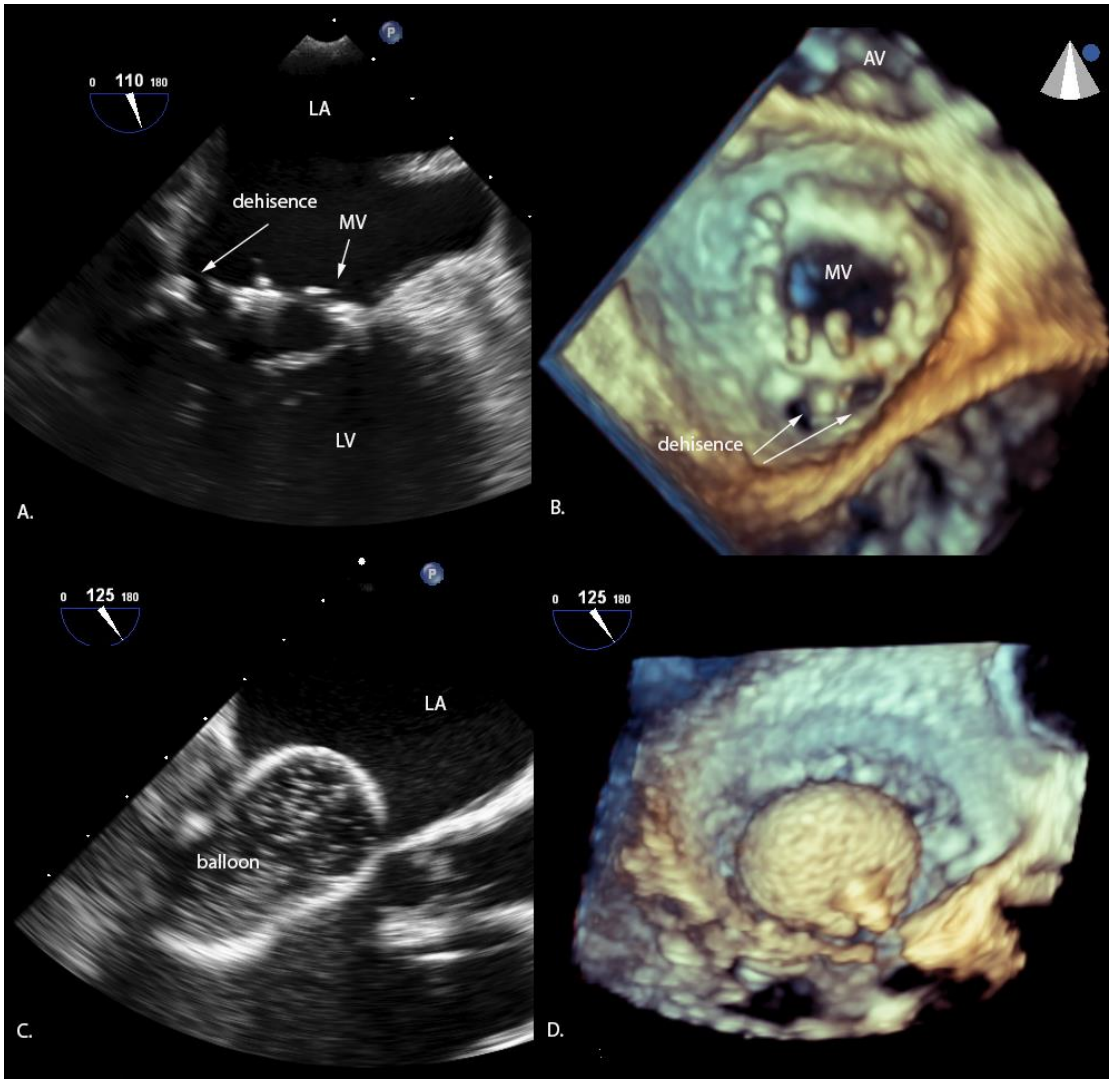


Figure 11. Mitral valve prosthesis valve dehiscence. Two-dimensional TEE image demonstrates a valve dehiscence adjacent to the mitral valve (MV) prosthesis (Panel A). Three-dimensional imaging in the same patient (Panel B), allows for improved spatial resolution with visualization of two defects adjacent to the lateral portion of the valve annulus (AV, aortic valve). In a different patient, TEE guidance allows for optimal placement of the MV valvuloplasty balloon during the procedure (2D, Panel C) (3D, Panel D).

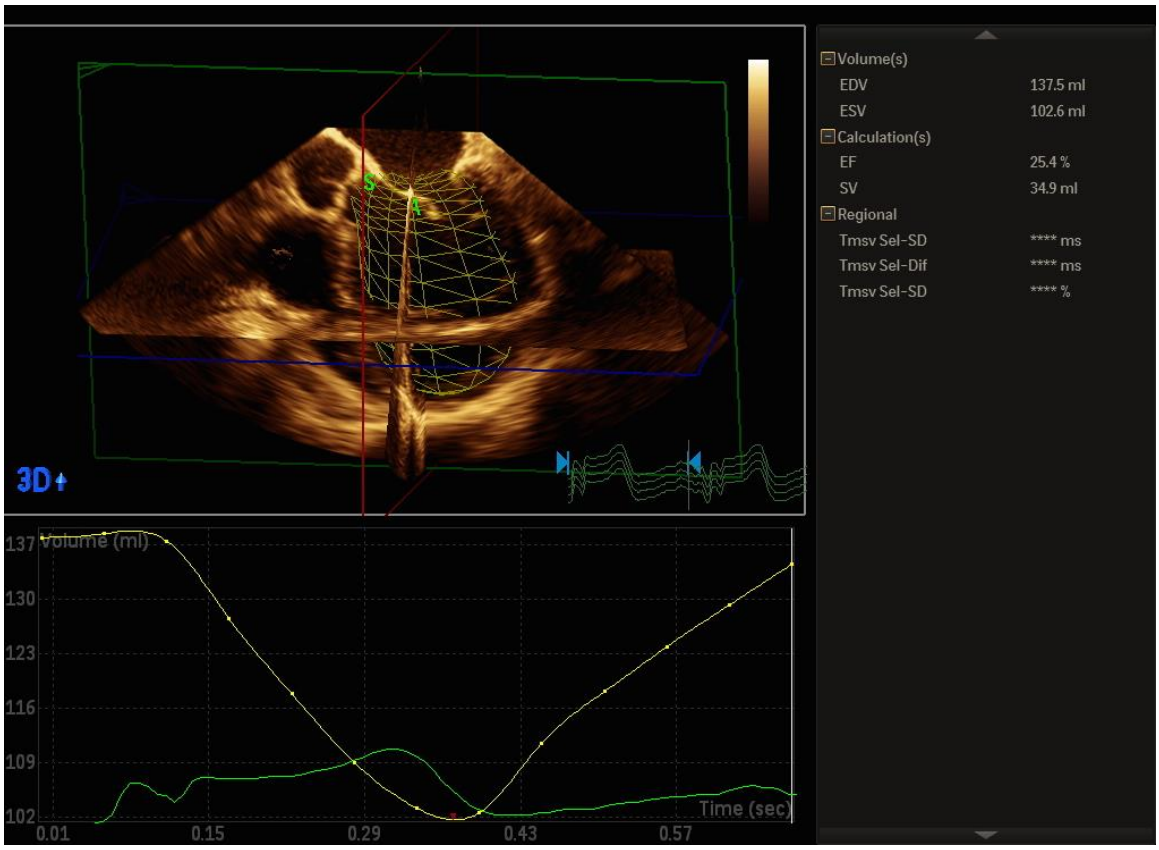


Figure 12. Three-dimensional evaluation of LV function. 3D end-diastolic volume (EDV) is 137mL and end systolic volume (ESV) is 103mL, with a stroke volume of 35mL, and calculated ejection fraction (EF) of 25%.

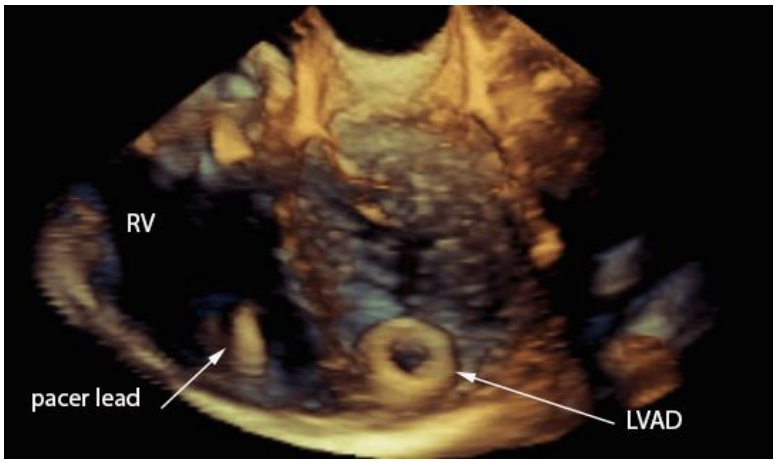


Figure 13. Three-dimensional imaging of a left ventricular assist device (LVAD) allows evaluation of septal motion relative to the inflow cannula in a patient where there was clinical suspicion for intermittent cannula obstruction due to suction events. Also shown is an RV pacer lead.

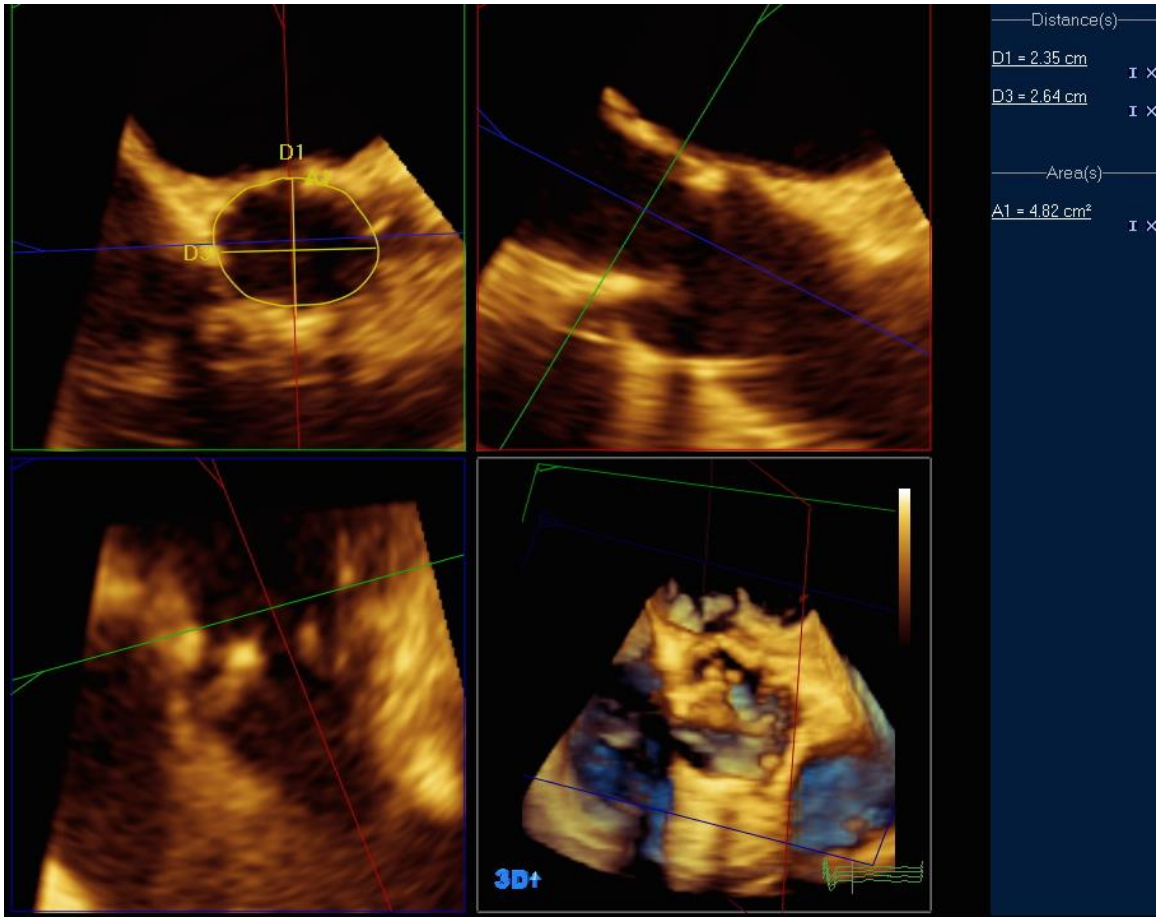

Figure 14. Three-dimensional imaging of the left ventricular outflow tract (LVOT) allows visualization of both the minor (D1) and major (D3) axes of the LVOT for optimal sizing of a transcatheter aortic valve prosthetic valve during the procedure.

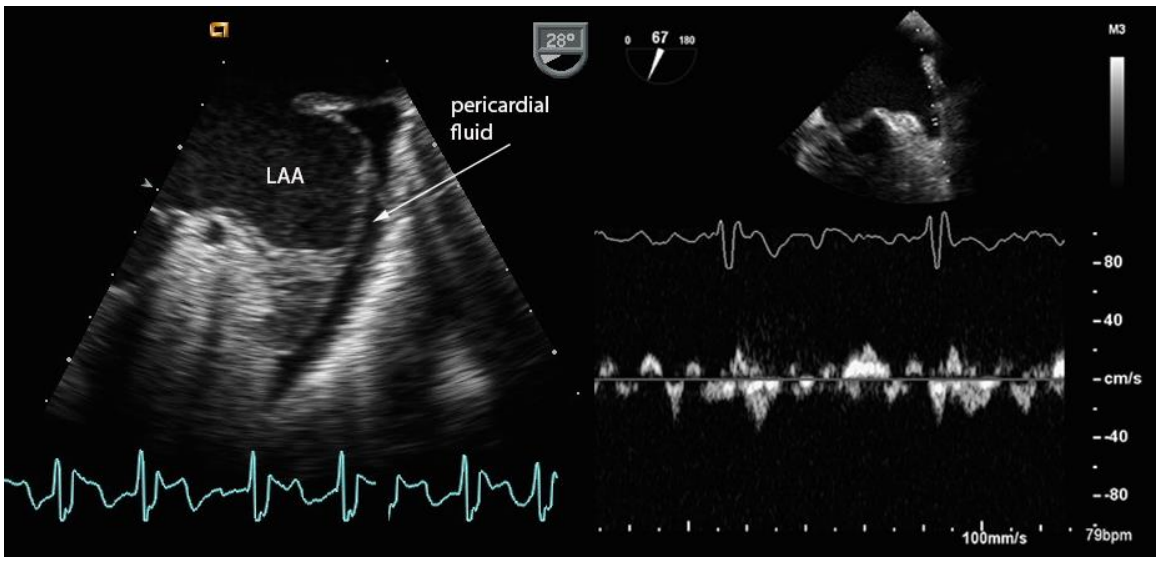


Figure 15. Left atrial appendage (LAA) thrombus filling the distal third of the appendage. Echolucent pericardial fluid adjacent to the appendage provides contrast between the pericardium and thrombus filled appendage (left). Pulse wave Doppler interrogation from the body of the left atrial appendage (right). The ECG tracing shows atrial fibrillation. Velocities in the appendage are decreased, at peak ~20cm/s.

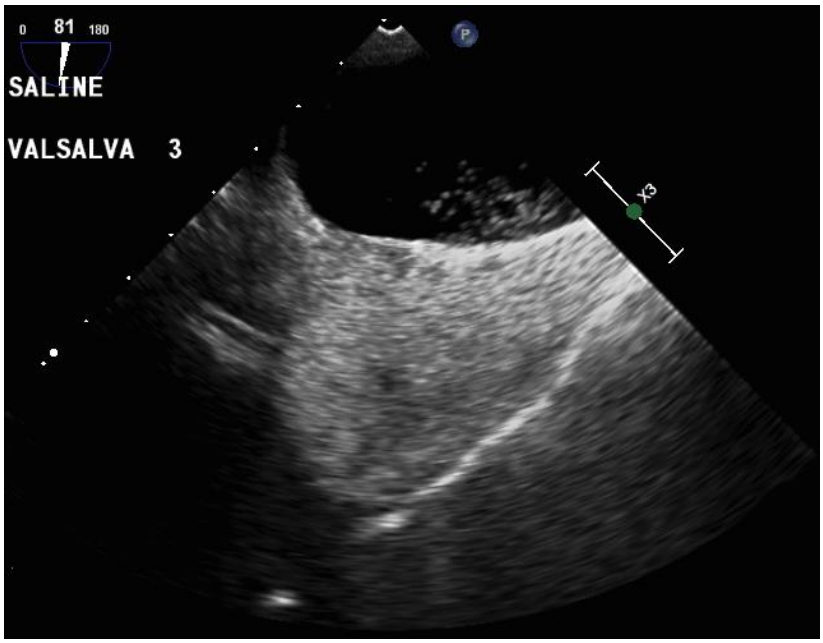


Figure 16. Agitated saline contrast study from [View 11] Mid-esophageal bicaval view. Agitated saline enters the LA from the SVC. Following Valsalva maneuver, a small amount of bubbles are seen just above the inter-atrial septum in the left atrium on the right hand side of the image after crossing a patent foramen ovale.

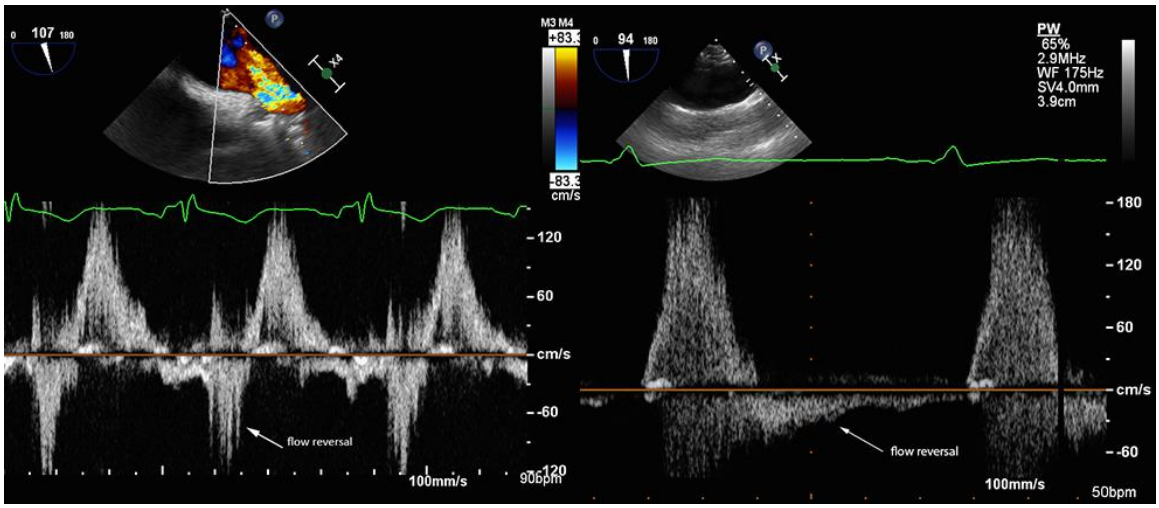


Figure 17 Spectral Doppler interrogation of the right upper pulmonary vein (left) in a patient with severe mitral regurgitation demonstrates systolic (as shown in the accompanying ECG tracing) reversal of flow with signal directed away from the transducer. In a patient with severe aortic regurgitation, Doppler interrogation of the thoracic aorta shows reversal of flow during diastole (right).

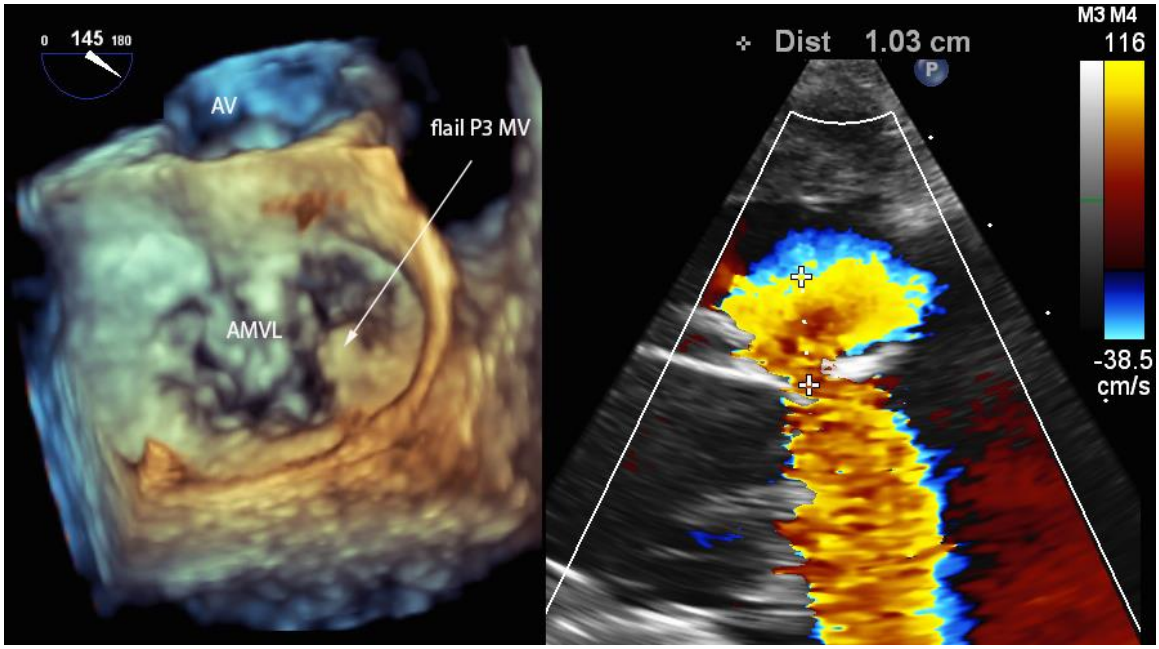


Figure 18. Severe mitral regurgitation. Enface view of the mitral valve via 3DE shows flail of the medial portion of the posterior mitral valve leaflet in the P3 segment (left). The regurgitant jet was eccentric and anteriorly directed due to the flail. With the color baseline moved in the direction of flow, away from the transducer, the aliasing velocity is 38.5m/s (right). At this aliasing velocity, the radius of the proximal isovelocity surface area measured 1.03cm.

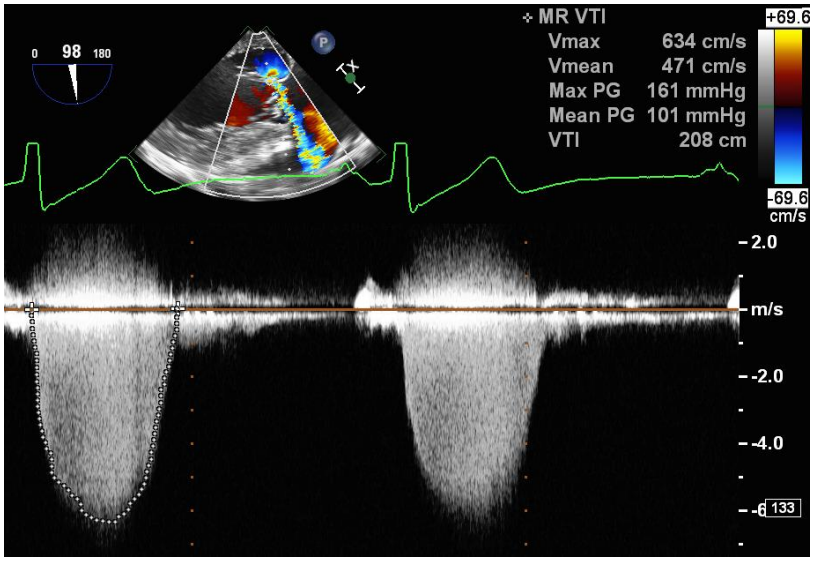


Figure 19. Severe mitral regurgitation. Continuous wave spectral Doppler tracing of the mitral regurgitant jet. Optimal alignment of the regurgitant jet was obtained from the transgastric long axis view (98°). The peak velocity is 634cm/s with velocity time integral (VTI) measurement 208cm. The effective regurgitant orifice area (EROA) calculation based on Figure 18 is ($2\pi r^2$ X aliasing velocity)/peak regurgitant velocity, or 0.4$cm^2$ consistent with severe mitral regurgitation. The EROA multiplied by the MR VTI provides a regurgitant volume of 84mL.

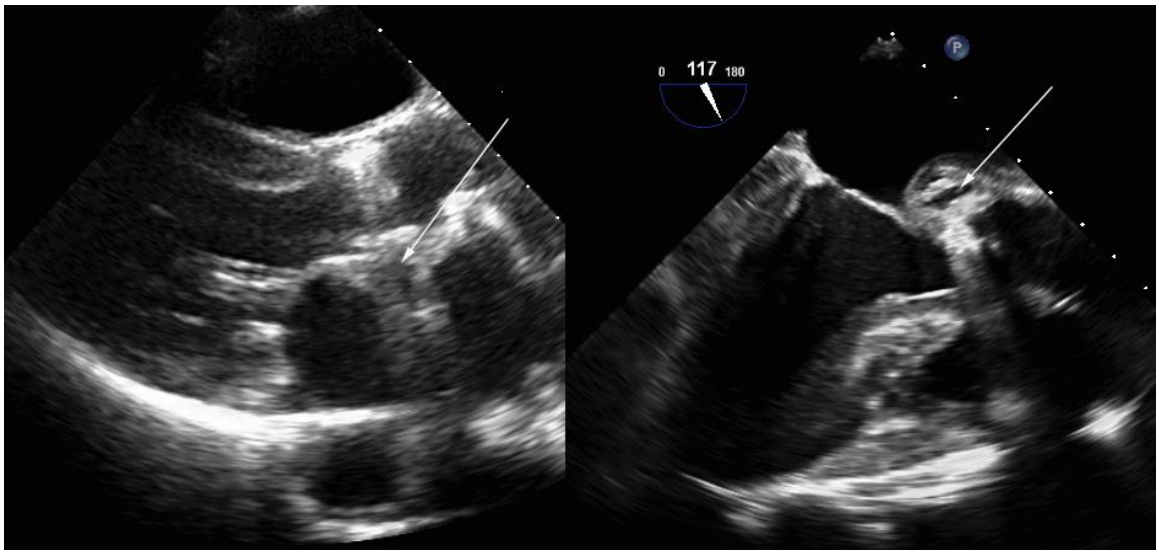


Figure 20. Paravalvular abscess. Transthoracic imaging of a mechanical aortic valve prosthesis from the parasternal long-axis view in a patient presenting with fatigue and elevated white blood cell count (left). Acoustic shadowing from the prosthesis precludes definitive evaluation of the posterior portion of the aortic valve annulus. Subsequent TEE imaging from [View 5] the mid-esophageal long axis view (117°) clearly demonstrates abnormal thickening adjacent to the prosthetic valve with central echolucency concerning for abscess (arrow, right).

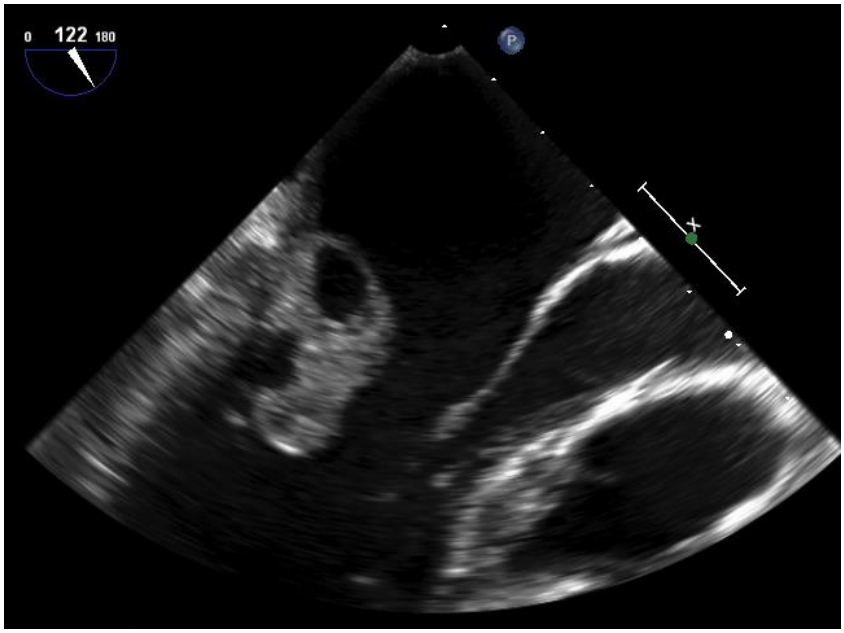


Figure 21. Large mitral valve vegetation encompassing the entire posterior mitral valve leaflet, as imaged from [View 5] the mid-esophageal left ventricular long axis view (122°). In this example, there is also a large region of echolucency consistent with abscess within the vegetation.

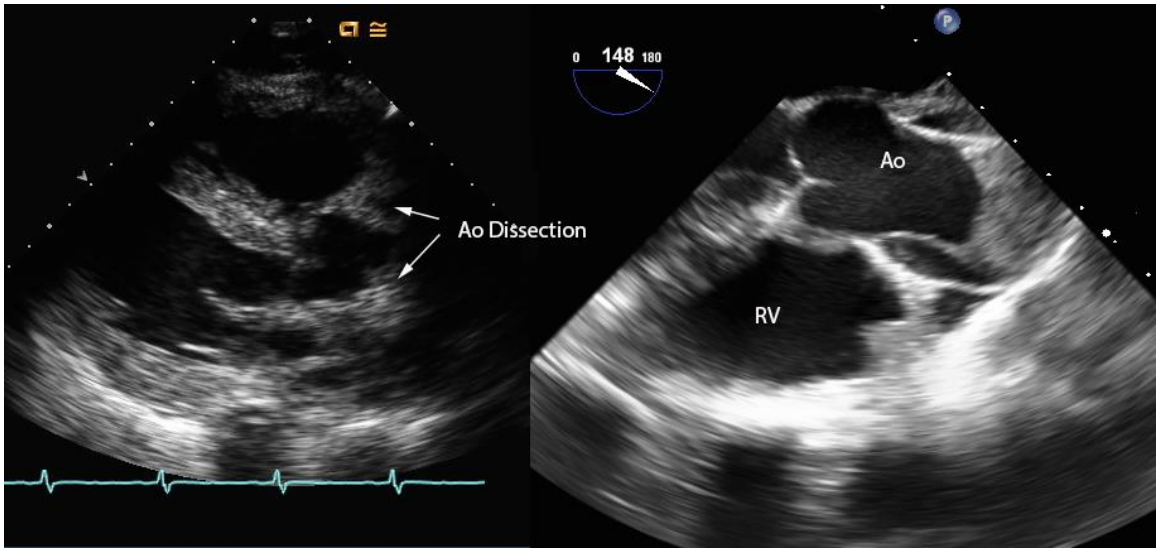


Figure 22. Ascending aortic dissection. Transthoracic imaging of an acute aortic dissection from the parasternal long-axis view in a patient presenting with sudden onset precordial and back pain (left), with poor visualization of the mid and distal ascending aorta. TEE imaging demonstrates the aortic dissection plane, with false lumen seen anterior and posterior to the true lumen, distal to the sinotubular junction (right).

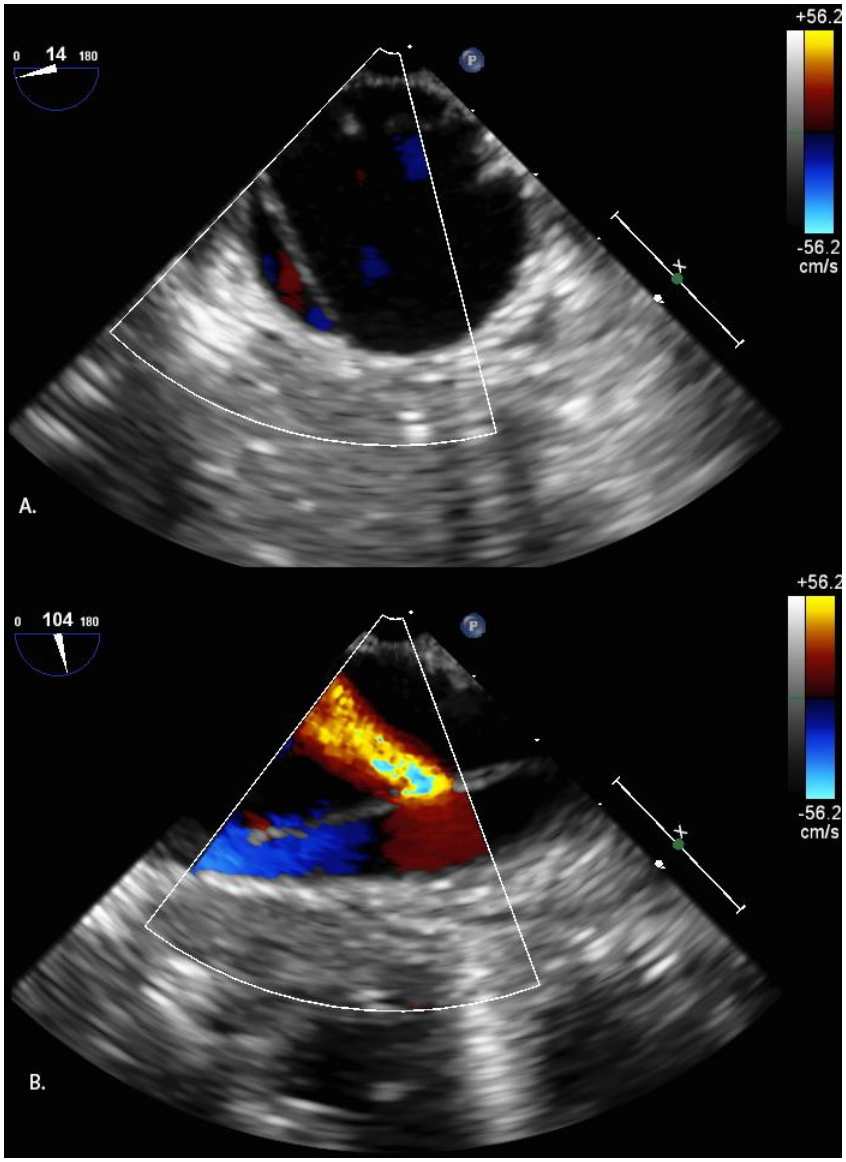

Figure 23. Descending thoracic aortic dissection. Mid-esophageal descending aorta short-axis view (14°)[View 25](top) shows the dissection flap along the left side of the image. The mid-esophageal descending aorta long-axis view (104°)[View 26](bottom) shows the orthogonal view of the dissection flap, with color Doppler allowing visualization of communication between the true and false lumen.

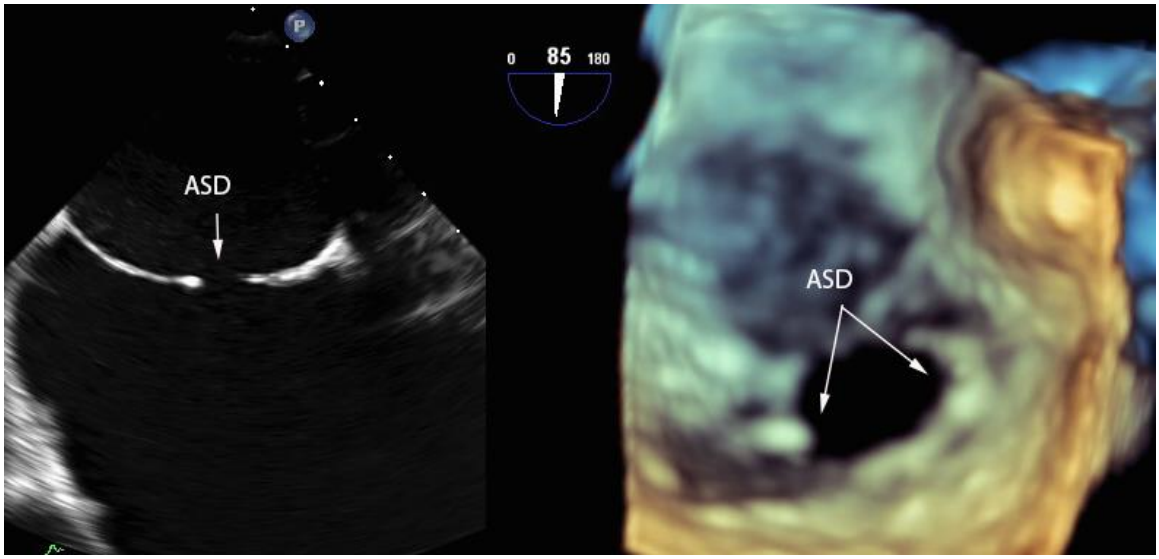

Figure 24. Secundum atrial septal defect. Two-dimensional imaging of the inter-atrial septum shows the defect. 3DE imaging in the same patient allows for improved visualization of the defect relative to other structures in the atrium as well as measurement of defect size.